Desalination and Water Treatment
www.deswater.com
5 (2009) 223–234

Stand-alone groundwater desalination system using reverse osmosis combined with a cooled greenhouse for use in arid and semi-arid zones of India

P.A. Davies[a]*, A.K. Hossain[a], P. Vasudevan[b]

[a]Sustainable Environment Research Group, School of Engineering and Applied Science, Aston University, Birmingham B4 7ET, UK
Tel. +44 121 204 3724; Fax: +44 121 204 3683; email: p.a.davies@aston.ac.uk
[b]Centre for Rural Development and Technology, Indian Institute of Technology, New Delhi 110 016, India

Received 24 August 2008; Accepted 17 December 2008

ABSTRACT

In many areas of northern India, salinity renders groundwater unsuitable for drinking and even for irrigation. Though membrane treatment can be used to remove the salt, there are some drawbacks to this approach e.g. (1) depletion of the groundwater due to over-abstraction, (2) saline contamination of surface water and soil caused by concentrate disposal and (3) high electricity usage. To address these issues, a system is proposed in which a photovoltaic-powered reverse osmosis (RO) system is used to irrigate a greenhouse (GH) in a stand-alone arrangement. The concentrate from the RO is supplied to an evaporative cooling system, thus reducing the volume of the concentrate so that finally it can be evaporated in a pond to solid for safe disposal. Based on typical meteorological data for Delhi, calculations based on mass and energy balance are presented to assess the sizing and cost of the system. It is shown that solar radiation, freshwater output and evapotranspiration demand are readily matched due to the approximately linear relation among these variables. The demand for concentrate varies independently, however, thus favouring the use of a variable recovery arrangement. Though enough water may be harvested from the GH roof to provide year-round irrigation, this would require considerable storage. Some practical options for storage tanks are discussed. An alternative use of rainwater is in misting to reduce peak temperatures in the summer. An example optimised design provides internal temperatures below 30°C (monthly average daily maxima) for 8 months of the year and costs about €36,000 for the whole system with GH floor area of 1000 m^2. Further work is needed to assess technical risks relating to scale-deposition in the membrane and evaporative pads, and to develop a business model that will allow such a project to succeed in the Indian rural context.

Keywords: Reverse osmosis; Photovoltaic; Concentrate disposal; Brackish water; Greenhouse

1. Introduction

Membrane processes based on reverse osmosis (RO) provide the most energy efficient method of desalination. For seawater, they typically require ten times less energy than thermal processes; for brackish groundwater the advantage is even greater. Due to the affordability, availability and low running costs of RO systems, the market for them will continue to expand and — as it does so — further technological improvements can be expected. Current research in this area includes, for example, the incorporation of chlorine groups into sulphonated

*Corresponding author.

Presented at the First UK–Israeli Workshop and Research Event on the Application of Membrane Technology in Water Treatment and Desalination, 15–20 June 2008, University of Oxford, UK.

polysulphone material to reduce biofouling, and the use of high-permeability pores made from carbon nanotubes that could eventually shave energy consumption towards the thermodynamic minimum [1].

There are, however, environmental problems associated with RO in particular when used for the treatment of groundwater. If too much water is extracted from an aquifer, contamination and salinisation may occur due to infiltration from surrounding water bodies and rocks [2]. Then at the outlet side of the RO plant, there is the problem of disposal of the reject water which can pollute surface waters and soils. For inland applications, the dearth of satisfactory disposal solutions has sometimes prevented altogether the construction and operation of RO plants [3]. This has prompted considerable interest in high-recovery systems using multiple stages and hybrid technologies, as reported by others at this meeting [4–6].

The present study has arisen in the context of a research project whose broad aim is sustainable development for people living in the drylands stretching west of Delhi. Preliminary fieldwork indicated that scarcity of energy and water resources are factors that hinder economic and social development, especially among rural communities whose only source of water is from brackish wells and the limited and seasonal rainfall. The need to invest in appropriate methods of making use of these resources in an environmentally-friendly manner is very apparent.

The technological intervention discussed here is guided by the following considerations: (1) if groundwater needs to be desalted, the preferred energy source should be local and renewable; (2) concentrate from the desalination process should be managed with minimal environment impact and preferably used to provide some valuable service; (3) freshwater produced should be for irrigation in as efficient a manner as possible; (4) it makes sense to use rainwater if available since this is an inherently renewable and free resource; and, most importantly, (5) the intervention as a whole should provide economic value and help alleviate poverty.

2. Proposed system

Greenhouses provide a water-efficient means of cultivation. Due to the humid and partially shaded area conditions, evapotranspiration inside a greenhouse (GH) is typically reduced by between 65% and 80% compared to outside [7]. In addition, GH cultivation is a high value activity, enabling a wide range of seedlings and crops to be raised at various times of year, thus providing additional opportunities for farmers [8]. Further, it has been found that salty water can be used satisfactorily in evaporative cooling systems for GHs, as required in hot climates [9].

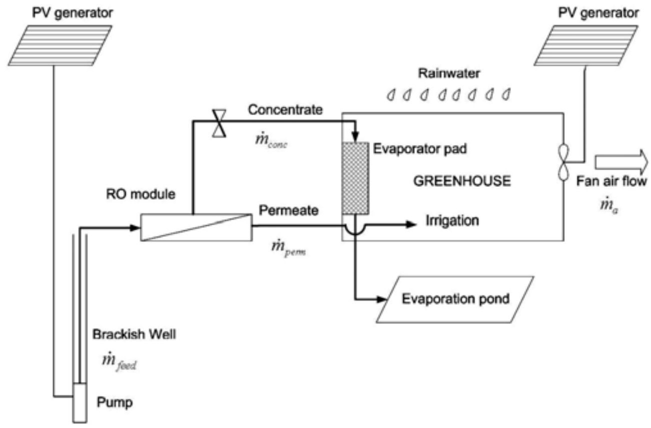

Fig. 1. Schematic of the proposed groundwater desalination system combined with a greenhouse.

The system proposed here, shown in Fig. 1, uses the product and reject water from an RO system to supply a GH with irrigation and cooling water respectively. The reject water is concentrated and reduced in volume, finally to be evaporated to solid in a pond. The solid salt could be disposed of as landfill therefore causing less of pollution than the liquid concentrate. Alternatively it could be used as a chemical feedstock for making products such as bleach. Given the high availability of sunlight in India, and the intermittency of the grid electricity supply, it is proposed to power the system using photovoltaics (PV). Finally, the roof of the GH will be used to collect rainwater, thereby supplementing the output from the PV–RO system.

The overall aim of this study is evaluate the feasibility of this concept. To achieve this, the following specific objectives are set: (1) to establish the optimal sizing of the PV-pump relative to the RO membrane, (2) to establish the appropriate sizing of the cooling system in relation to the GH, (3) to consider the matching between a PV-powered desalting system and the cooled GH, and (4) to quantify the additional contribution to irrigation from rainwater harvesting. These objectives will be met through the application of simple models for the various system components. As a result, we will indicate the technical performance and costs of the system. In addition we will comment on technical risks and the scope for further investigation. The study has been carried out for the target area in the vicinity of Delhi.

3. Optimal design of the PV-powered desalting system

There are many practical examples of RO systems that operate from renewable energies and PV in particular, using both seawater and brackish water. Costs in the range of 2.5 to 10 €/kWh have been reported [10]. Most such systems use PV or wind turbines, or a combination of the two, together with battery banks. However, for irrigation use the water demand is expected to be closely related to the amount of sunlight and this makes it attractive to consider a system without batteries since these are typically among the least durable components. The design of battery-less PV–RO systems has been studied in detail and demonstrated by Thomson and Infield [11,12].

The choice of pump is one of the first points to consider in such a system. Centrifugal pumps are widely available and inexpensive, but poorly suited to operation at the varying power inputs as will be needed in the battery-less system due to the variation in sunlight intensity. The pressure developed will fall off rapidly with rotation speed making it difficult to meet the minimum pressure requirements of the RO process other than under full sunlight. Positive displacement pumps, though generally more expensive and less readily available, are much more flexible in providing varying combinations of pressure and flow. From an energy point of view, the Clarke pump (as used by Thomson and Infield for example) is ideal as it recoveries energy from the concentrated stream; but here we are particularly interested in choosing a pump that is suited to operation in boreholes used to access groundwater. Therefore, a progressive cavity (Moineau) pump has been selected. Such pumps are available as complete PV-powered systems. By specifying a single pump giving sufficient pressure to lift the water out of the borehole and supply the membrane directly, we can avoid the need for two pumps.

We now consider the optimal relative sizing of the PV-pump and RO elements of the system. A convenient and conventional way to describe the size of the PV-pump is by peak power ($\hat{P}_{\mathrm{PVpump}}$), meaning the total electrical power output, under the standard solar irradiance of 1000 Wm^{-2} (1 sun), of the PV panels used to drive the pump. The size of the membrane will be measured according to its area A_{mem}. Typically the membranes are spiral wound inside cylindrical vessels and a number of such elements can be connected together to obtain the required area.

3.1. Model equations

An approximate model has been developed based on mass and energy balance, and on standard equations representing transport across the RO membrane in terms of two properties: the permeability coefficient to water, S, and the salt transport coefficient B [13]. The discharge Q_{perm} of water permeating the membrane and the mass flow $\dot{m}_{\mathrm{salt}}$ of salt across it are given by:

$$Q_{perm} = A_{mem} S(\Delta p - \Delta p_{osm}) \tag{1}$$

and

$$\dot{m}_{salt} = A_{mem} B \Delta c \tag{2}$$

where A_{mem} is the membrane area; while Δp, Δp_{osm} and Δc represent respectively the total driving pressure, osmotic pressure difference and the difference in salt concentration across the membrane. The value of Δp_{osm} will be based on the mean concentration c_{wall} of dissolved salts at the membrane wall which increases along the length of the vessel as some of the feed water permeates through the membrane. It also increases due to concentration polarisation. The ratio $\alpha = c_{wall}/c_{feed}$ is used to represent these increases. Based on reference [14],

$$\alpha = \frac{1 + 1/(1-r)}{2} \exp(0.7r) \tag{3}$$

where r is the recovery ratio. For the purpose of calculating both Δc and Δp_{osm}, the permeate is taken to be virtually salt free; thus $\Delta c = c_{wall}$.

The hydraulic power P_{pump} needed of the pump equals the pressure rise it develops multiplied by the discharge from it. Assuming that the pressure on the permeate side of the membrane is atmospheric, and taking into account the depth d of the well, we obtain based on Eq. (1):

$$P_{pump} = \frac{Q_{perm}}{r} \left(\Delta p_{osm} + \rho_w g d + \frac{Q_{perm}}{A_{mem} S} \right) \tag{4}$$

At this point it is useful to introduce a simple model for the cost $\mathbf{C}_{\mathrm{des}}$ of the desalination system, as follows.

$$\mathbf{C}_{des} = \hat{P}_{PVpump} C_{PVpump} + A_{mem} C_{mem} \tag{5}$$

where C_{PVpump} is the cost per peak watt of PV-pump, and C_{mem} is the cost per area of membrane. In practice, the flow and power inputs will be time-varying; however, the optimisation will be presented based on typical operating conditions. The PV-pump will normally be working at a power level below $\hat{P}_{PVpump}$; therefore, a capacity factor $\kappa < 1$ can be used to represent its average daytime power level. In calculating P_{pump} we must also consider the overall efficiency η, accounting for losses in the motor, pump and pipework. Then:

$$P_{pump} = \eta \kappa \hat{P}_{PVpump} \tag{6}$$

Elimination of P_{pump} and $\hat{P}_{PVpump}$ among Eqs. (4)–(6) and differentiation with respect to A_{mem} yields the following approximate result for the value of average flux Q_{perm}/A_{mem} that will result in the minimum system cost $\mathbf{C}_{des}$.

$$\frac{Q_{perm}}{A_{mem}} = \sqrt{r\kappa\eta S \frac{C_{mem}}{C_{PVpump}}} \tag{7}$$

It is interesting that this gives an optimum flux that is independent of well depth and osmotic pressure, and therefore of the salt concentration in the feed. We also need to consider that a lower value of flux tends to result in a higher salt concentration in the permeate, and this places a constraint [based on Eq. (2)] on the minimum flux needed to maintain C_{perm} below a threshold level:

$$\frac{Q_{perm}}{A_{mem}} \geq B\alpha \frac{C_{feed}}{C_{perm}} \tag{8}$$

The flux chosen should therefore be the higher of these two values.

3.2. Choice of data

From data sheets provided by the manufacturer, the values of B and S for three commonly used membranes were deduced and are shown in Table 1. As regards membrane costs, for all types the retail price was found to be about €80, including the cost of the membrane vessels which were chosen to be 2.5" diameter by 40" long. Information was obtained from manufacturers of PV-pumping systems with regard to costs based on a system with $\hat{P}_{PVpump}$ =450 W, and is included in Table 2.

Regarding typical capacity factor κ and operational day length, we note from Lorenzo [15] that 90% of solar energy is received during the period centred around noon of duration equal to two thirds the day length, regardless of location and time of year. Therefore, we assume an average operational day length of 8 h. Analysis of the weather data for Delhi shows that the average global solar irradiation on the horizontal within this period averages approximately 550 Wm^{-2}, giving κ = 0.55 [16].

Table 1
Properties of example membranes considered in this study

Type	Manufacturer's code	Permeability S m s^{-1}Pa^{-1}	Salt transport coefficient B m s^{-1}
Low energy	XLE-2540	2.2×10^{-11}	1.2×10^{-7}
Brackish water	BW30-2540	1.0×10^{-11}	5.9×10^{-8}
Seawater	SW30-2540	4.1×10^{-12}	6.3×10^{-8}

Table 2
Parameters used in the model of the PV-powered desalination system. Currency conversion rates used: €1 = 1.6 Australian dollars = 1.55 US dollars = 0.79 GB pounds = 66 Indian Rupees.

Membrane cost C_{mem}, € m^{-1}	80
PV-pump cost C_{PVpump}, € W^{-1}	12
PV-pump system efficiency, η	0.59
Capacity factor	0.55
Maximum salt concentration in permeate c_{perm}, ppm	500
Well depth d, m	0

Further data as needed to apply to the model, including that obtained from the manufacturer of the PV-pump, are given in Table 2. To calculate Δp_{osm} as a function of c_{feed}, it is necessary to know the ionic composition of the feed water which is site specific. For generality the results given here are for sodium chloride solutions, this typically being the most abundant salt.

3.3. Results

Based on the foregoing equations and data, Table 3 gives examples of optimal designs giving an average daily output of 1 m^3 of desalted water, for different values of c_{feed}, r and d. For larger or smaller outputs, the figures in Table 3 may be scaled proportionately as long as C_{mem} and C_{PVpump} remain constant, which is a reasonable assumption in the sense that both RO and PV are modular technologies having only modest economies of scale.

Except for the highest values of c_{feed} and r shown, the governing constraint on flux is cost [based on Eq. (7)] rather than concentration of salt in the output stream [based on inequality (8)]. In all cases, the preferred membrane is the low energy type 1. Peak operating pressures are calculated to remain well within specified limits for the membranes in all cases.

The optimal flux is in the range at 3–5×10^{-6} ms^{-1} (11–18 Lm^{-2} h^{-1}), which is around 30% of the levels typically used in conventional applications. This reflects the fact that the PV-pump is a relatively costly energy source, and the economic membrane size is therefore large to minimise pumping power. Fig. 2 illustrates that, at these low fluxes, water output is approximately proportional to power input. Note that the cost of the PV-pump is from 2.4 to 8 times that of the membrane.

Fig. 3 indicates the sensitivity of the system cost to the relative sizing, $A_{mem}/\hat{P}_{PVpump}$. Initially, increasing the relative membrane area decreases system cost as energy input is lowered, but then it becomes unjustified to add further membrane and the system cost increases slightly. Note however that, around the minimum, the system cost is not very sensitive to sizing and that practical choices

Table 3
Optimised desalination systems giving an output of 1 m^3/d on average, with salinity below 500 ppm, for different feedwater salinities and recovery rates, showing the sizes and costs of the PV-pump and RO components

System	Well depth (d), m	Feed salinity, (c_{feed}), ppm	Recovery rate (r)	Flux (Q_{perm}/A_{mem}), ms^{-1a}	Sizes		Costs, €		
					PV-pump ($\hat{P}_{PVpump}$), W	RO (A_{mem}), m^2	PV-pump	RO	Total
1	0	2,000	0.2	3.1	181	11.2	2,170	900	3,070
2	0	2,000	0.35	4.1	133	8.5	1,590	680	2,270
3	0	2,000	0.5	4.9	117	7.1	1,410	570	1,970
4	0	5000	0.2	3.1	340	11.2	4,080	900	4,980
5	0	5,000	0.35	4.1	247	8.5	2,960	680	3,640
6	0	5,000	0.5	4.9	222	7.1	2,660	570	3,230
7	0	10,000	0.2	3.1	606	11.2	7,270	900	8,170
8	0	10,000	0.35	4.1	437	8.5	5,240	680	5,920
9	0	10,000	0.5	5.0	398	6.9	4,780	550	5,330
10	10	5,000	0.2	3.1	393	11.2	4,710	900	5,610
11	10	5,000	0.35	4.1	277	8.5	3,320	680	4,000
12	10	5,000	0.5	4.9	243	7.1	2,920	570	3,480

[a] $1\ ms^{-1} = 3.6\ Lm^{-2}\ h^{-1}$.

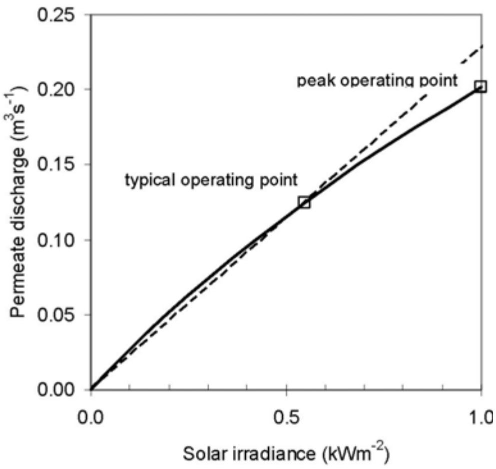

Fig. 2. Water output of the PV-powered RO system is approximately proportional to solar power input. Solid lines plot discharge of permeate against solar irradiance with c_{feed}=5000 ppm, r = 0.35, d = 10 m, A_{mem}= 0.85 m^2, η = 0.59, $\hat{P}_{PVpump}$ = 277 W. Broken line shows linear approximation.

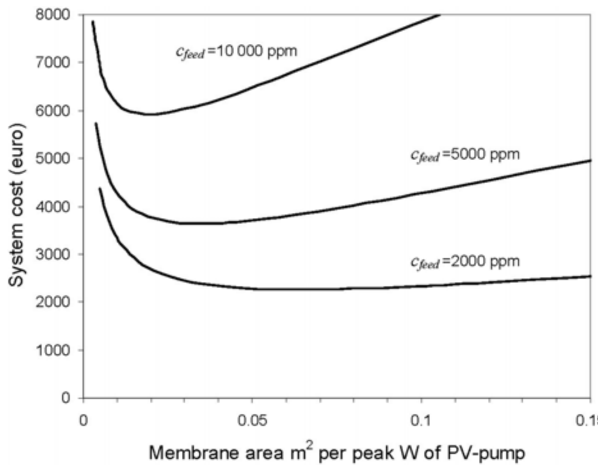

Fig. 3. Optimal sizing of the RO membrane relative to the PV-pump occurs when the system cost is minimized. The system cost for 1 m^3/d output of desalted water is plotted against the membrane area per peak W ($A_{mem}/\hat{P}_{PVpump}$) for different levels of feed water salinity c_{feed}.

will be affected by the need to use integral numbers of PV and RO modules.

The contribution of membrane replacement costs has not been included in the calculation. We would expect the cost per replacement to increase with membrane area, but that replacement would occur less often as fouling would be slower at the lower flux. In this sense it is reasonable to assume that membrane replacement costs do not affect the optimal choice of sizing.

3.4. Verification against manufacturer's predictions

Manufacturers of membranes typically make available public domain software for the prediction of RO system performance. The applicable software package (ROSA© version 6.1.5) has been used to analyse a system similar to that proposed here, based on row 5 in Table 3. An array of three elements in parallel (low energy type as in Table 1), has been specified, giving a single pass through a total membrane area of 7.8 m^2. This is slightly smaller than the

Table 4
Prediction using ROSA© of the performance of a system similar to that of row 5 in Table 3, consisting of a single pass arrangement of three low energy type elements in parallel (see Table 1)

Feed salinity based on NaCl, ppm	5000
Total membrane area (A_{mem}), m^2	7.8
Flux (Q_{perm}/A_{mem}), μms^{-1} (Lm^{-2}h^{-1})	4.5 (16)
Permeate flow, L h^{-1}	3.5×10^{-5} (125)
Pump electrical power input, W:	
Average	140
Peak	255
Recovery	0.35
Feed pressure, bar	8.2
Permeate salinity based on NaCl, ppm	292

optimum value of 8.5 m^2 shown in Table 3. The predictions from ROSA are summarised in Table 4. The smaller area of membrane results in a slightly higher feed pressure and in a peak power requirement of 255 W, compared to only 247 W in Table 3 where membrane area is treated as a continuously variable parameter without the constraint of having to use a whole number of elements. Otherwise there is no important difference between the software predictions and the results obtained using the model equations above. Note that ROSA predicts a permeate salinity of 292 ppm.

4. Appropriate sizing of the greenhouse and its cooling system

We now consider the sizing of the GH together with the cooling system consisting of the PV-fan and evaporative pads. A larger cooling system will provide lower temperatures, allowing the GH to be used for a greater fraction of the year without overheating. It will also cost more, however, and increasing the size of the cooling system will provide diminishing returns as the internal temperature approaches the ambient wet-bulb temperature, this being the lowest temperature that can ordinarily be achieved by the fan-and-pad cooling arrangement discussed here.

The measure of temperature adopted is the average daily maximum for each month of the year, this being one that is commonly used in describing climates around the world and that is useful in assessing suitability for any particular crop. The appropriate range of temperature for GH cultivation is crop specific but generally lies in the range 20 to 30°C [17]. Temperate crops such as lettuce require temperatures at the lower end of this range, while subtropical crops such as tomato and cucumber can tolerate higher temperatures up to 32 or even 35°C [18]. In Fig. 4 we see the average daily maxima for wet- and dry-bulb temperatures in Delhi. The highest wet-bulb

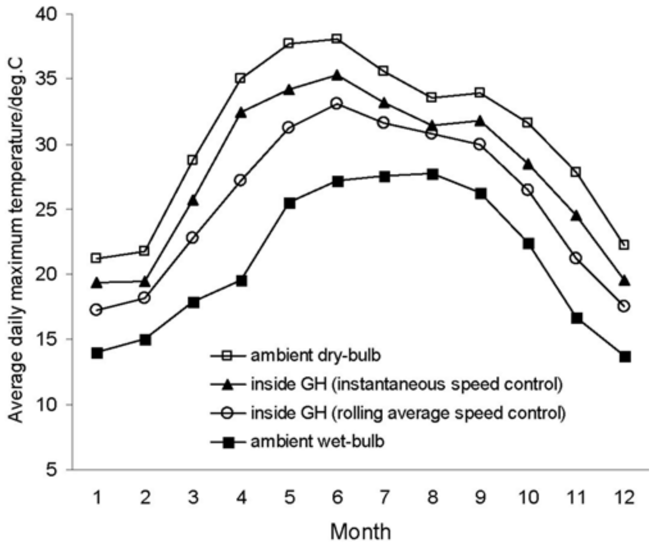

Fig. 4. Method of controlling fan speed in response to sunlight affects the efficacy of cooling. Instantaneous speed control is compared and with control based on a rolling average of irradiance over last 4 h (ms^{-1}). Ambient temperatures are also shown based on ISHRAE [16].

temperatures occur from June to August when they often exceeding 27°C. This is therefore the period when adequate cooling is most difficult to achieve.

4.1. Model equations

Kittas et al. [19] have provided a validated model of a cooled GH that will be adopted here. This model uses a one-dimensional heat balance approach to represent the temperature gradient between the evaporative pads where the air enters and the fan where it leaves. Integration over this gradient gives the following expression for the spatial average of internal temperature:

$$T_{avg} = T_{dry} + T_{\max} + \left[-\varepsilon\left(T_{dry} - T_{wet}\right) - T_{\max}\right] \cdot\theta\cdot\left[1 - \exp(-1/\theta)\right] \tag{9}$$

where T_{wet} and T_{dry} are the ambient wet- and dry-bulb temperatures respectively and ε is the effectiveness of the evaporative cooling pads. The symbol $T_{\max}$ represents the temperature rise above T_{dry} that would theoretically occur in the GH in the absence of air flow, given by:

$$T_{\max} = \frac{\tau(1-\beta)R}{K\gamma} \tag{10}$$

where t is the transmissivity of the GH cover, β is the fraction of incoming solar radiation absorbed as latent heat as opposed to sensible heat, R is the global solar irradiance on the horizontal, K is the heat transfer coefficient of the GH cover and γ is the ratio of the perimeter of the GH cover along a cross section perpendicular to the air flow, divided by the width measured on the same cross section. The term θ is a function of the air flow through the GH:

$$\theta = \frac{v\rho_a c_p}{K\gamma} \tag{11}$$

where v represents the specific ventilation rate (units ms^{-1}) which is equal to the volumetric air flow V divided by the floor area A_{GH} of the GH. The size of the PV-powered cooling system is represented by its peak air flow capacity $\hat{V}$, as achieved under standard conditions of $\hat{R}$ = 1000 Wm^{-2}, and corresponding to this there is a peak value $\hat{v}$ of v. Now the power consumption of a fan varies with the cube of the speed [20]. Therefore:

$$v = \hat{v} \cdot \sqrt[3]{R/\hat{R}} \tag{12}$$

The cost $\mathbf{C}_{coolGH}$ of the cooled GH will be

$$\mathbf{C}_{coolGH} = \hat{V} C_{PVcool} + A_{GH} C_{GH} \tag{13}$$

where C_{PVcool} is the cost of the PV-powered cooling system, per m^3s^{-1} of peak air flow capacity, and C_{GH} is the cost of the GH structure per m^2 of floor area.

4.2. Choice of data

The physical data used in this model are that provided by Kittas, as shown in Table 5 (where a choice of values is provided a mean has been taken). The cost data for the GH and PV-powered cooling system were taken from current prices of off-the-shelf components used. In Davies et al. [21], it was shown that a GH ventilation system can be constructed with energy usage as low as 20 J per m^3 of air moved, and this has been taken as the basis for the sizing and costing of the PV generators in the system. The model has been applied to the weather data for Delhi on an hour-by-hour basis [16].

Table 5
Parameters used in the model of the cooled GH. Currency conversion rates used are as in Table 2

Roof transmission, τ	0.5
Latent heat fraction, β	0.5
Ratio of perimeter to width, γ	1.2
Effectiveness of the evaporators, ε	0.8
Heat transfer coefficient K, W $m^{-2}K^{-1}$	4.2
Cost of the cooling system C_{PVcool}, € m^{-3} s	360

4.3. Results

Table 6 shows how the temperature inside the GH will vary with the choice of peak specific ventilation rate $\hat{v}$. It also shows the cost of the cooling system on the basis of a GH of floor area 1000 m^2. As the peak ventilation rate $\hat{v}$ is increased from 0.01 to 0.035 ms^{-1}, the benefit of cooling increases significantly, lengthening the period for which average daily maxima are kept below 30°C from 3 to 8 months of the year. Above this ventilation rate, however, little further benefit is obtained while the cost of the cooling system continues to increase in proportion to $\hat{v}$. At $\hat{v}$ = 0.035 ms^{-1} the average daily maximum temperature exceeds 32°C in the month of July only. This is therefore taken as an appropriate level of ventilation.

5. Matching the desalination system to the cooled GH

Having discussed separately the design of the desalination system and the cooled GH, we are now able to consider the matching between the two. The output of desalted water needs to match the irrigation requirement of the crop while the output of concentrate needs to match that needed to supply the evaporative pads of the cooling system.

If irrigation is applied efficiently with negligible run-off, it can be calculated based on evapotranspiration. The classical model due to Penman and later improved by Monteith [22] considers two components of evapotranspiration — the first driven by solar radiation and the second by vapour deficit. The second component is usually much smaller and, especially for the sunny and humid conditions inside a GH, is reasonably neglected [19]. In this case the rate of evapotranspiration $\dot{m}_{evap}$ is proportional to solar radiation.

$$\lambda \dot{m}_{evap} = \tau \beta R A_{GH} \tag{14}$$

where λ is the latent heat of vapourisation of water. For the climate of Delhi, and using the same values of τ and β as before, this yields an average evaporation rate of 1.8 mm/d inside the GH. Since the water output of the PV-powered desalination system is also approximately proportional to the solar radiation, supply follows demand, and there is hardly any need for storage. Sizing becomes a matter of equating average water output and irrigation usage throughout the year. On this basis, the desalination systems described in Table 3 (with an output of 1 m^3/d) will irrigate a GH with an area of 560 m^2. For convenience we shall now base our discussions on a GH of

Table 6
Effect of ventilation rate on the average daily maximum temperatures (°C) inside the cooled GH for each month of the year as a function of the size of the cooling system, also showing the cost of the cooling system on the basis of a GH of size A_{GH}=1000 m^2, to be compared with the cost of the GH structure estimated at €15.000. Recommended design is shown in bold type

Peak specific ventilation rate $\hat{v}$ ms^{-1}	Month 1	2	3	4	5	6	7	8	9	10	11	12	Cost of cooling system (A_{GH}= 1000 m^2) €
0.01	21.7	22.6	28.1	32.7	37.1	38.0	36.6	35.8	35.8	32.5	27.0	22.6	3600
0.02	18.7	19.6	24.3	28.0	32.6	34.0	32.9	32.4	31.8	28.4	23.1	19.2	7200
0.03	17.6	18.5	23.1	27.3	31.5	33.2	31.8	31.1	30.4	26.9	21.6	17.9	10800
0.035	**17.3**	**18.2**	**22.8**	**27.2**	**31.3**	**33.1**	**31.6**	**30.8**	**30.0**	**26.5**	**21.2**	**17.6**	**12600**
0.04	17.0	18.0	22.6	27.2	31.2	33.0	31.5	30.6	29.7	26.1	20.9	17.3	14400
0.06	16.5	17.6	22.2	27.1	30.9	32.8	31.4	30.1	29.2	25.4	20.2	16.7	21600
0.08	16.2	17.4	22.1	27.1	30.9	32.7	31.3	29.9	29.0	25.1	19.9	16.4	28800

GH temperature (avg. daily max)
>32 cultivation difficult or impossible
30-32 cultivation possible but not optimal
20-30 optimal range for many crops
<20 cooling excessive or not needed

1000 m^2, therefore requiring a system 1.8 times the size of those in Table 3. Note that although this calculation is for Delhi, if the system were located elsewhere with lower or higher insolation, about the same area could be irrigated using the same equipment, as both supply and demand would vary in proportion to the insolation available.

With regard to the concentrate water fed to the cooling system, the matching is less straightforward as output depends on solar radiation whereas usage depends on humidity. The water must be supplied at a rate that makes up for evaporation with some excess corresponding to the outflow to the evaporation pond. Some such outflow is necessary to prevent salt build up on the evaporative pads. If the volume of concentrate leaving is a fraction μ of that entering, then the mass flow of concentrate water needed for cooling is:

$$\dot{m}_{conc} = \frac{\dot{m}_a \varepsilon \left(\phi_{wet} - \phi_{dry}\right)}{1 - \mu} \tag{15}$$

A mass balance calculation has been carried out for the year on an hourly basis, assuming β = 0.1, meaning that the concentrate volume is reduced 10-fold. This calculation shows that the rate of recovery needed to give a net balance of zero over the whole year is r = 0.33. However, this results in a mismatch at different times throughout the year, as seen in Fig. 5 where the mass balance has been presented for each month. Evaporation increases sharply in the spring, due to high ambient temperatures and low humidity, leading to a shortage of water for cooling.

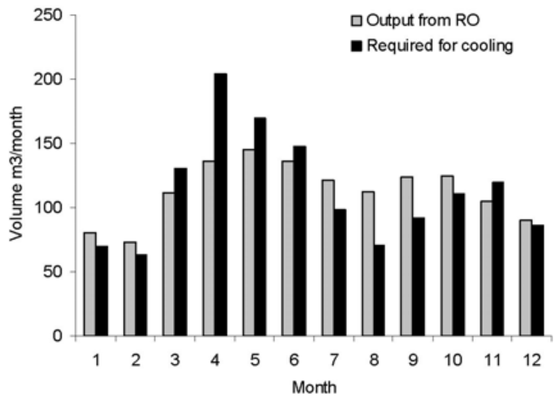

Fig. 5. At constant recovery rate there is a mismatch between concentrate output from the RO and the water required for cooling system. The histogram compares monthly supply and demand for A_{gh} = 1000 m^2 and r = 0.33, which is the recovery ratio needed to give a net balance of zero over the whole year.

To eliminate this mismatch whilst avoiding the need to store large amounts of concentrate, two approaches have been considered. The first is to run the reverse osmosis system at a sufficiently low and constant recovery rate to provide enough cooling water even for April, which is the month where most is needed, and to oversize the cooling system so that it is capable of running at higher airflows to evaporate the excess concentrate when least is needed in August. This results in a recovery rate r = 0.25 and an increase of 50% in the size of the cooling system at an additional expense of about €6000 based on the 1000 m^3 GH size.

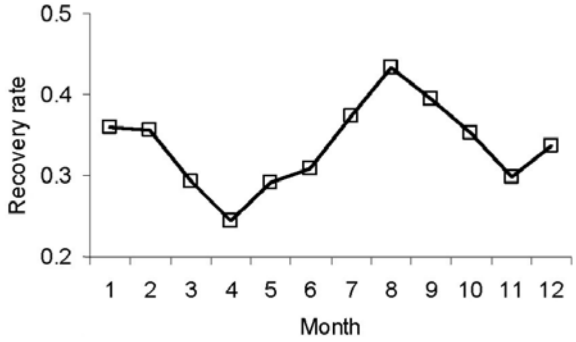

Fig. 6. Recovery rates needed to supply desalted water for irrigation and concentrate water for cooling in the requisite proportions for each month.

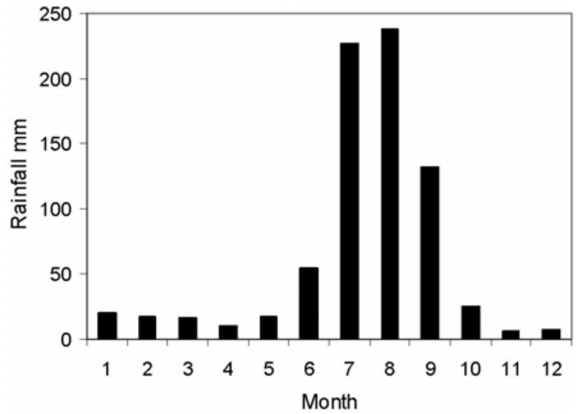

Fig. 7. Normal rainfall in Delhi for each month of the year [23].

The alternative is to design a variable recovery rate RO system that can provide greater or smaller amounts of concentrate at different times of year. This would mean that the recovery rate should vary between r = 0.25 (in April) to r = 0.44 (in August) as shown in Fig. 6. A system with appropriate sizing of PV generator and membrane area to give this range of r is estimated to cost €1300 more than the fixed recovery rate system and this is therefore the more cost-effective option (based on c_{feed}=5000 ppm and A_{gh}=1000 m^2).

6. Rainwater harvesting

The system proposed above will be self-sufficient in water, provided the groundwater is not depleted through over-extraction. Harvesting of rainwater from the GH roof may be considered as a means of reducing or avoiding this risk. Since the roof is already provided, the additional costs arise from the gutters, down pipes and storage tanks [24].

To help investigate this option, normal monthly rainfall data for New Delhi is presented in Fig. 7. Most rain falls from June to August, though the last week of May also sees significant rain if the monsoon arrives early as it did in 2008, and the receding monsoon gives significant rain in September, tapering off in October. Some precipitation occurs from November to February also, but these winter rains tend to be sparse and unpredictable. The long-term average rainfall for Delhi is nearly 800 mm per year. However, in 2006 and 2007 rainfall was only 619 and 602 mm respectively [23]. For the purpose of calculations, 600 mm will be taken as representative of a lean monsoon.

In general, not all the water that falls on a roof is collected as some is retained and subsequently evaporates. However, a GH is usually a smooth structure as compared to, say, a tiled roof and therefore can be expected to achieve good collection efficiency — a figure of 80% is assumed. On this basis, the 1000 m^2 GH will collect about 640 m^3 of water during an average year, and 480 m^3 during a lean monsoon year. These figures compare to an irrigation requirement of 657 m^3 per year based on the 1.8 mm daily requirement estimated above. In principle, then, rainwater can provide most of the irrigation required over the year. However, as noted earlier, the requirement for cooling is twice this amount. One solution would be to supply cooling water from a brackish well and to irrigate with rainwater held in storage tank — perhaps topping up the irrigation water with brackish water in years of low rainfall. In this arrangement the cost and maintenance of the RO system would be avoided completely.

The drawback, however, is that a large and hermetic tank would be required to store most of the harvested water from the rainy season to provide for the other months. A volume of approximately 400 m^3 would be needed in this example.

Different practical options for tank construction can be considered. One is to install a ferrocement tank at a depth of 1 to 3 m underground within the GH itself, with a pump to draw water from the bottom. The cost is estimated to be €15/m^3, giving €6000 for a 400 m^3 tank. This is about 40% the cost of a GH structure and approaches the cost of the PV-powered desalination system; moreover, a borehole pump will still be needed to supply the cooling water. A potentially more cost-effective option would be to excavate the floor area under the GH structure to about 2 m depth, line with an impermeable plastic sheet and refill with sand and soil to provide an artificial aquifer. Taking sand and soil porosity into account, such a tank could store about 600 m^3 of rain water. It is possible that capillary action would be sufficient to draw the water up through the soil, eliminating the need for an irrigation pump. However, this needs to be verified experimentally. Further work is also needed to determine the correct depth of the plastic sheet.

Table 7
Rainfall in mm per day in Delhi since January 2007 (source IARI New Delhi)

Day	2007												2008					
	Jan	Feb	Mar	Apr	May	Jun	Jul	Aug	Sep	Oct	Nov	Dec	Jan	Feb	Mar	Apr	May	Jun
1	0	0	19	0	0	0	0	0	0	0	0	0	0	0	0	1	0	0
2	0	0	0	0	0	0	0	16	0	0	0	0	0	0	0	0	0	0
3	0	0	0	0	1	0	0	12	3	0	0	0	0	0	0	1	0	0
4	0	0	0	0	0	0	8	10	24	0	0	0	0	0	0	0	0	0
5	0	0	0	0	0	0	3	18	0	0	0	0	0	0	0	24	0	6
6	0	0	0	0	0	0	0	0	0	0	0	0	0	0	0	5	0	0
7	0	0	0	0	6	0	0	0	0	0	0	0	0	0	0	0	0	0
8	0	0	0	0	0	0	0	0	0	0	0	0	0	0	0	0	0	0
9	0	0	0	0	0	0	0	0	0	0	0	0	0	0	0	0	0	0
10	0	0	0	0	0	0	0	3	35	0	0	0	2	0	0	0	0	0
11	0	31	0	0	2	0	0	0	2	0	0	0	0	0	0	0	5	0
12	0	2	9	0	11	0	0	0	0	0	0	0	0	0	0	0	0	0
13	0	15	15	0	0	0	13	9	0	0	0	0	0	0	0	0	0	0
14	0	6	0	0	0	0	27	0	0	0	0	0	0	0	0	0	0	33
15	0	0	0	0	0	0	4	0	0	0	0	0	0	0	0	0	22	3
16	0	0	0	0	0	26	11	0	0	0	0	0	0	0	0	0	0	27
17	0	0	0	0	15	5	0	0	0	0	0	0	0	0	0	0	0	14
18	0	0	0	0	0	22	0	0	0	0	0	0	0	0	0	0	2	6
19	0	0	0	0	0	2	0	0	0	0	0	0	0	0	0	0	7	2
20	0	0	0	0	0	0	0	1	0	0	0	0	0	0	0	0	10	0
21	0	0	12	0	0	0	0	0	0	0	0	0	0	0	0	0	40	1
22	0	0	0	0	0	0	0	0	0	0	0	0	0	0	0	0	21	0
23	0	0	0	0	0	0	0	0	0	0	0	0	0	0	0	0	28	0
24	0	0	0	0	0	0	1	0	0	0	0	0	0	0	0	0	0	4
25	0	15	0	0	0	0	14	0	0	0	0	0	0	0	0	0	0	0
26	0	15	0	0	0	25	0	0	2	0	0	0	0	0	0	0	0	0
27	0	14	0	0	4	4	0	0	0	0	0	0	0	0	0	0	2	0
28	0	3	0	0	0	0	0	3	0	0	0	0	0	0	0	0	0	2
29	0	—	0	0	3	0	1	0	7	0	0	0	0	0	0	0	0	0
30	0	—	0	0	0	0	0	0	0	0	0	0	0	—	0	0	0	0
31	0	—	0	—	0	—	0	0	—	0	—	0	0	—	0	—	0	—

An alternative use for rainwater would be in a misting system to produce peak temperatures in the hot, rainy months of June, July and August. The temperature can rise by 5 or 6°C between the air inlet and outlet of the GH, and misting could be used to counteract this, as it would provide cooling along the GH length. Misting works by absorbing the incoming solar energy as latent rather than sensible heat; in other words, the value of β in Eq. (10) is increased. The water requirements for misting will therefore be of the same order as for evaporative cooling. Table 7 shows daily rainfall patterns in Delhi since January 2007. From this it can be seen that it is unusual to have more than 7 consecutive dry days once the monsoon has started. On this basis it is estimated that storage of about 20 m^3 would be sufficient for misting in the GH of floor area 1000 m^2.

7. Conclusions and further work

A simple method for the optimal sizing of the elements of a PV-powered RO desalination system has been presented and applied for the Delhi climate. The first step is to calculate the optimal membrane flux, which is essentially independent of well feed concentration and well depth, and lies in the range 3 to 5 $\mu m\ s^{-1}$ (11–18 $L m^{-2} h^{-1}$). At such low fluxes the water output is approximately proportional to solar energy input and to evapotranspiration. Therefore the water output can be matched to the irrigation requirement without the need for significant storage of water or energy.

In using the concentrate output to supply an evaporative cooling system of a GH, however, the supply of water is not matched to evaporation because the latter depends on humidity, not sunlight. This mismatch can be overcome by using a RO system with a recovery rate varying from 0.25 to 0.44 over the year. Using a PV-powered fan with peak specific ventilation rate of 0.035 ms^{-1}, it is practical to cool the GH so as to achieve internal temperatures (ie. average daily maxima) below 30°C for 8 months of the year, providing suitable growing conditions for many crops, and to below 32°C for every month except June when temperatures reach 33°C.

Table 8 summarises these findings to give the performance and costs of the main components, based on an example with A_{GH}=1000 m^2, c_{feed} = 5000 ppm and d = 10 m. The total cost is about €36,000, of which 41% corresponds to the GH structure, 24% to the desalination system and 35% to the GH cooling system. Additional costs occurring in a real project, such as those of the land and the well, are not included here because they are very site specific. Rainwater harvested from the GH roof could be used to provide additional cooling through misting in summer months, but the additional cost of implementing this has not been included in Table 8.

The use of harvested rainwater for irrigation becomes competitive with the desalination system if a large storage tank can be constructed at low cost, but does not provide enough water for greenhouse cooling. These costs are based mainly on global sources of components. For a project in India it may be possible to reduce costs by local sourcing of, for example, the GH structure. Other specialized elements such as the PV generators are likely to remain expensive in the short term. In the long term innovations in PV technology using thin films based on amorphous silicon–hydrogen alloys or polycrystalline compound semi-conductors, perhaps integrated with the GH cover material, could lead to significant cost reductions [25].

In order to balance water requirements for irrigation and cooling, the recovery rate suggested here averages 0.33 over the year. Note however that in modern RO systems recovery rates of 0.5 or higher are achievable [6]. The concept proposed could usefully be combined with such high-recovery systems if some of the desalted water were diverted for non-irrigation purposes such as drinking.

This study has focused on the conceptual design of a PV-powered RO system that irrigates and cools a GH. There remain significant technical challenges to overcome in implementing such a concept in detail. Deposition of insoluble salts on the membrane and evaporative cooling pads could deteriorate performance, requiring the addition of descaling chemicals with possible cost and environmental implications. Alternatively, innovations in materials specifically designed for air-drying of concentrate as reported at this meeting could provide a solution [5]. Another approach may be to use a nanofiltration membrane pre- or post-treatment stage to remove divalent ions responsible for scaling [4].

Apart from the technical challenges, there are many social and business challenges to overcome for the concept to become viable. The capital costs are large for most Indian rural communities and would require a significant external investment. This will require a business plan to be developed, for which this technical study will provide an important input.

Table 8
Main features of an example recommended design for greenhouse floor area A_{GH}=1000 m^2 providing the temperatures as shown in Table 5 for $\hat{v}$ =0.035 ms^{-1}.

Sizes:		
GH floor area A_{GH}, m^2		1000
PV pump: peak electrical power $\hat{P}_{PVpump}$, W		607
RO membrane area A_{mem}, m^2		18
GH cooling system: peak air flow, $m^3 s^{-1}$		35
Well depth d, m		10
Water input and output:		
Flow of feed water from well[a], m^3/d		5.4
Salinity of feed water, ppm		5000
Flow of desalted water for GH irrigation[a], m^3/d		1.8
Salinity of irrigation water, ppm		<500
Flow of concentrate water from RO[a], m^3/d		3.6
Flow of concentrate after volume reduction[a], m^3/d		0.36
Salinity of concentrate after volume reduction[a], ppm		75,000
Costs, €:		
GH structure		15,000
Desalination system:		8,730
	PV-powered pump	7,280
	RO membranes	1,450
GH cooling system		12,600
Total		36,330

*Yearly average.

8. Symbols

- A — Area, m^2
- B — Salt transport coefficient, ms^{-1}
- c — Salt concentration, ppm
- C — Cost per unit of size, €
- $\mathbf{C}$ — Cost, €
- c_p — Specific heat capacity of air, J $kg^{-1}K^{-1}$,
- d — Well depth, m
- g — Acceleration due to gravity, ms^{-2}
- K — Heat transfer coefficient for GH cover, $Wm^{-2}K^{-1}$
- $\dot{m}$ — Mass flow rate, kgs^{-1}
- p — Pressure, Pa
- P — Power associated with pump, W

Q — Discharge of water, m^3s^{-1}
r — Recovery rate
R — Solar irradiance, Wm^{-2}
S — Permeability to water, $ms^{-1}Pa^{-1}$
T — Temperature, K or °C
v — Specific ventilation rate, V/A_{gh}, ms^{-1}
V — Flow of air, m^3s^{-1}

Greek

α — c_{wall}/c_{feed}
β — Latent heat fraction
γ — Ratio of GH perimeter (in cross section) to width
ε — Effectiveness of evaporative pad
η — Efficiency of PV-pump system
θ — Dimensionless form of *v*
κ — Capacity factor
λ — Latent heat of vaporisation of water, J kg^{-1}
μ — Volume fraction to which concentrate is reduced
ρ — Density of water, kg m^{-3}
τ — Transmissivity of GH cover to sunlight
ϕ — Absolute humidity, kg kg^{-1}

Subscripts and embellishments
a — Air
avg — Spatial average
conc — Concentrate
coolGH — Cooled greenhouse
des — Desalination system
dry — Dry bulb
feed — Feed water
GH — Greenhouse
mem — Membrane
osm — Osmotic
perm — Permeate water
pump — Pump
PVcool — PV-powered cooling system
PVpump— PV-powered pump system
salt — Salt
w — Water
wall — At membrane wall
wet — Wet bulb
^ — Peak value corresponding to full sunlight

Acknowledgements

The authors thank the other participants for their suggestions and feedback during and following this research. They also acknowledge funding from the Engineering and Physical Sciences Research Council, grant reference EP/E044360/1.

References

[1] R. Service, Desalination freshens up, Science, 313 (2006) 1088–1090.
[2] B.L. Morris, A.R.L. Lawrence, P.J.C. Chilton, B. Adams, R.C. Calow and B.A. Klinck, Groundwater and its susceptibility to degradation: A global assessment of the problem and options for management. Early Warning and Assessment Report Series, RS. 03-3. UN Environment Programme, Nairobi, Kenya, 2003.
[3] M. Mickley, Concentrate management, in: The Guidebook to Membrane Desalination Technology, M. Wilf, ed., Balaban, 2007.
[4] R. Singh, Brine recovery at industrial reverse osmosis plant — conceptual process design studies, 2nd Oxford Water and Membranes Research Event, Oxford, 2008.
[5] J. Gilron, Hybrid processes for high recovery from desalination of brines, 2nd Oxford Water and Membranes Research Event, Oxford, 2008.
[6] R. Singh, Hybrid Membrane Systems for Water Purification: Technology, Systems Design and Operations, Elsevier, Amsterdam, 2005.
[7] C. Fernandes, J. Cora and J. Campos de Araujo, Reference evapotranspiration estimation inside greenhouses, Scientia Agricola, 3 (2003) 591–594.
[8] B. Singh and N. Sirohi, Protected cultivation of vegetables in India: problems and future prospects, Acta Horticulturae, 710 (2006) 339–342.
[9] P.A. Davies and C. Paton, The Seawater Greenhouse in the United Arab Emirates: thermal modeling and evaluation of design options, Desalination, 173 (2005) 103–111.
[10] E. Tzen, Desalination units for portable water production, 2nd International Conference on Small and Decentralised Wastewater Treatment Plant, Skiathos, Grafima, 2008.
[11] M. Thomson and D. Infield, A photovoltaic-powered seawater reverse-osmosis system without batteries, Desalination, 153 (2003) 1–8.
[12] M. Thomson and D. Infield, Laboratory demonstration of a photovoltaic-powered seawater reverse-osmosis system without batteries, Desalination, 183 (2005) 105–111.
[13] M. Wilf, The Guidebook to Membrane Desalination Technology, Balaban, 2007.
[14] FILMTEC Reverse Osmosis Membranes Technical Manual, Dow Chemical Company, 2005.
[15] E. Lorenzo, Solar Electricity, Progensa, 1994.
[16] ISHRAE, India Weather Data Set 2005, Indian Society of Heating Refrigerating and Air-Conditioning Engineers.
[17] J. Hanan, Greenhouses: Advanced Technology for Protected Horticulture, CRC Press, Boca Raton, 1998, Chap. 4.
[18] R. Hochmuth, Florida Greenhouse Vegetable Production Handbook, Vol. 3, http://edis.ifas.ufl.edu [accessed 9th January 2006].
[19] C. Kittas, T. Bartzanas and A. Jaffrin, Temperature gradients in a partially shaded large greenhouse equipped with evaporative cooling pads, Biosystems Eng., 86 (2003) 87–94.
[20] F. Bleier, Fan Handbook, McGraw Hill, New York, 1997, Chap. 5.
[21] P.A. Davies, A.K. Hossain, G. Lychnos and C. Paton, Energy saving and solar electricity in fan-ventilated greenhouses, Acta Horticulturae, 797 (2008) 339–346.
[22] J.L. Monteith and M.H. Unsworth, Principles of Environmental Physics, Edward Arnold, 1990.
[23] IARI, http://www.iari.res.in/ [accessed 29th July 2008].
[24] T.H. Thomas and D.B. Martinson, Roofwater harvesting — a handbook for practitioners, Technical Paper Series 49, IRC Int. Water and Sanitation Centre, Delft, 2007.
[25] M.A. Green, Recent developments in photovoltaics, Solar Energy, 76 (2004) 3–8.